ELSEVIER

Catalysis Today 50 (1999) 63–71

CATALYSIS TODAY

Influence of the acidity of USY zeolite on the sulfur tolerance of Pd–Pt catalysts for aromatic hydrogenation

Hiroyuki Yasuda*, Toshio Sato, Yuji Yoshimura

National Institute of Materials and Chemical Research, Tsukuba, Ibaraki 305-8565, Japan

Abstract

A series of bimetallic Pd–Pt (mole ratio Pd : Pt = 4 : 1) catalysts supported on HY and USY (ultrastable Y) zeolites for a wide range of SiO_2/Al_2O_3 ratio (5.6–680) was prepared and characterized by chemical analysis, XRD, N_2 adsorption, IR spectroscopy of pyridine adsorption, and CO adsorption. The hydrogenation of tetralin was done over the Pd–Pt/HY and Pd–Pt/USY catalysts at a hydrogen pressure of 3.9 MPa at 553 K in the presence of dibenzothiophene at a sulfur concentration of 500 ppm. The hydrogenation activity, selectivity, and the sulfur tolerance strongly depended on the SiO_2/Al_2O_3 ratio of the zeolites. The activity increased with increasing SiO_2/Al_2O_3 ratio, peaked when the ratio was in the 15.0–40 range, and then decreased as the ratio increased further. The IR analysis showed that for the USY zeolites with a SiO_2/Al_2O_3 ratio of 15.0 or above, the amount of Brønsted acid sites was extremely small, while strong Lewis acid sites existed on the surface of these zeolites. The decrease in both the activity and the sulfur tolerance of Pd–Pt/USY catalysts when the SiO_2/Al_2O_3 ratio increases from 15.0–40 to 680 may be primarily due to the decrease in the amount of electron-deficient Pd–Pt resulting from the decrease in Lewis acidity. Compared with the Pd–Pt/USY (SiO_2/Al_2O_3 = 15.0–40) catalysts, the activities of the Pd–Pt/HY and Pd–Pt/USY (SiO_2/Al_2O_3 = 10.7) catalysts were lower, probably because of pore diffusional limitations.

Keywords: Aromatic hydrogenation; Sulfur tolerance; Pd–Pt catalysts; USY zeolites; Acid sites in USY

1. Introduction

Deep hydrogenation of aromatics in diesel fuel is now receiving considerable attention because aromatic compounds are recognized as being related to the formation of diesel particulates in the exhaust gases, as well as to the reduction of fuel quality [1,2]. For the hydrogenation of aromatics, lowering the reaction temperature will be necessary not only for economical reasons but also for increasing the yield and the stability of the hydrogenated products. Although noble metal catalysts are highly active for the hydrogenation of aromatics, noble metals are generally poisoned easily even by a few parts per million of sulfur in the feedstock [3,4]. Therefore, the sulfur content in feedstock must be strictly reduced before such catalysts come in contact with the feedstock.

Recently, for the hydrogenation of aromatics, much attention has been paid to the high sulfur tolerance of Pd, Pt, and bimetallic Pd–Pt catalysts supported on various supports, including Al_2O_3, TiO_2, and acidic zeolite [5–11]. Pd–Pt/USY (ultrastable Y) catalysts

*Corresponding author. Tel.: 81-298-54-4530; fax: 81-298-54-4532; e-mail: yasuda@nimc.go.jp

0920-5861/99/$ – see front matter
PII: S0920-5861(98)00463-5

are also active for the hydrodesulfurization [12]. We previously reported that the activity and the sulfur tolerance of Pd–Pt/USY ($SiO_2/Al_2O_3 = 680$) catalysts for the hydrogenation of tetralin in the presence of dibenzothiophene (DBT) strongly depended on the Pd : Pt ratio, and that a maximum activity was obtained when the mole ratio Pd : Pt = 4 : 1 [13]. However, little is known about the influence of the acidity of the supports on the hydrogenation activity and on the sulfur tolerance of Pd–Pt.

In this study, we therefore prepared a series of bimetallic Pd–Pt (mole ratio Pd : Pt = 4 : 1) catalysts supported on HY and USY zeolites for a wide range of SiO_2/Al_2O_3 ratio (5.6 to 680). We then investigated the influence of zeolite acidity on tetralin hydrogenation activity and selectivity as well as on the sulfur tolerance of Pd–Pt.

2. Experimental

USY zeolites (Tosoh, SiO_2/Al_2O_3 was 10.7 or 15.0, hereafter abbreviated as HY-10.7 and HY-15.0) were used as received. HY-15.0 was further de-aluminated by treatment with various hydrochloric acid concentrations (0.01–2 mol dm^{-3}), temperatures (298–373 K), and times (2–24 h). After the treatment, the de-aluminated zeolite was filtered, washed with water until no chloride ions were detected in the filtrate, and then dried at 383 K overnight. HY zeolite (hereafter abbreviated as HY-5.6) was prepared from NaY zeolite (Tosoh, $SiO_2/Al_2O_3 = 5.6$). NaY was ion-exchanged using an aqueous solution of ammonium nitrate at 298 K for 24 h, filtered, and then washed with water. This ion-exchange procedure was repeated three times. The ion-exchanged zeolite was then dried at 383 K overnight and calcined at 773 K for 2 h.

The bimetallic Pd–Pt catalysts supported on zeolites were prepared by incipient wetness impregnation with a mixed aqueous solution of $[Pd(NH_3)_4]Cl_2$ and $[Pt(NH_3)_4]Cl_2$. The mole ratio Pd : Pt was fixed at 4, and the total amount of metal loading was 1.2–1.3 wt.%. The impregnated sample was dried in vacuum at 333 K for 6 h, pressed into a wafer, crushed into 22/48 mesh chips, and then calcined in an oxygen stream (2 dm^3 min^{-1} g^{-1}) at 573 K for 3 h at a heating rate of 0.5 K min^{-1}. The precalcined sample was reduced in situ in a hydrogen stream before being used in the reaction or in the measurement of the metal dispersion.

The SiO_2/Al_2O_3 ratio of each zeolite was determined using an inductively coupled plasma spectrometer (ICP) (Seiko Instruments, SPS1200A). The unit cell constant and the crystallinity were determined using a X-ray diffractometer (Mac Science, M18XHF[22]). The unit cell constant was calculated from the 2θ values of 997 and 999 reflections. Silicon powder was used as an internal standard for determining 2θ values. The crystallinity was calculated from the average area of 533 and 642 reflections using NaY as the reference. The nitrogen adsorption isotherm of each zeolite was measured at 77 K using an automatic apparatus (Bel Japan, BELSORP 28SA) after the sample was evacuated at 773 K for 1 h. The total and mesopore surface areas were calculated using BET-plots and *t*-plots, respectively.

The dispersion of Pd–Pt on zeolites was determined by carbon monoxide (CO) adsorption measurements. The stoichiometry of CO to either Pd or Pt was assumed to be unity. The precalcined sample (50 mg) was pretreated in a hydrogen stream (30 cm^3 min^{-1}) at 573 K for 1 h, followed by purging by helium at the same temperature for 10 min. After the pretreatment, a CO pulse was injected into the sample several times at room temperature. The amount of CO uptake was measured by a thermal conductivity detector.

Infrared spectra (IR) of adsorbed pyridine on zeolites were measured at room temperature using an IR spectrometer (Shimadzu, FTIR-8200PC) and a quartz IR cell connected to a vacuum system. Prior to the measurements, the self-supporting sample wafer (40 mg) was evacuated at 723 K for 1 h. The spectrum was measured after a sample was exposed to pyridine (4 Torr) at 423 K for 15 min and evacuated at the same temperature for 15 min. The temperature was then increased stepwise to 573 and 723 K, and spectra were measured after the sample was evacuated for 15 min at each temperature. IR spectra from the adsorbed pyridine were obtained by subtracting the spectrum of the pretreated sample from the spectra obtained after adsorption.

The hydrogenation of tetralin was done in a high-pressure fixed-bed continuous-flow reactor (316 stainless steel tube, 1/6 in. i.d. and 0.6 m long), as described previously [13]. The liquid feed was a mixture of

tetralin (30 wt.%), DBT (0.3 wt.%, sulfur concentration of 500 ppm), and *n*-hexadecane (69.7 wt.%). The reaction conditions were a hydrogen pressure of 3.9 MPa, reaction temperature of 553 K, feed flow rate of 4 g h^{-1}, hydrogen flow rate of 2.46 dm^3 h^{-1}, catalyst weight of 0.25 g, and weight hourly space velocity (WHSV) of 16 h^{-1}. The volume ratio of hydrogen (NTP) to feed was 500. Prior to catalytic testing, the precalcined sample was treated in a hydrogen stream (100 cm^3 min^{-1}) at 101.3 kPa at 573 K for 3 h. The liquid products of the reaction were periodically collected and analyzed using a gas chromatograph (GC) (Shimadzu, GC-17A) equipped with a flame ionization detector and a capillary column (Hewlett-Packard, Ultra 1, 0.2 mm i.d. and 50 m long). The products were also analyzed using a GC (Hewlett-Packard, 5880A) and a mass selective detector (MS) (Hewlett-Packard, 5970).

3. Results

3.1. Physical properties of USY zeolites

Table 1 lists the results for the unit cell constant, crystallinity, and the total and mesopore surface areas of HY-5.6 and USY zeolites. Also listed are the conditions used in treating HY-15.0 with hydrochloric acid. Both the framework and nonframework aluminum species were eliminated by the acid leaching, and the SiO_2/Al_2O_3 ratio determined by a chemical analysis widely varied, from 15.9 to 680. The acid leaching caused the partial destruction of zeolite crystallites, resulting in a slight decrease in crystallinity. Furthermore, the acid leaching caused the formation of mesopores [14]. As a result, the mesopore surface area significantly increased from 19 m^2 g^{-1} to 71 m^2 g^{-1} when the SiO_2/Al_2O_3 ratio increased from 5.6 to 15.0, and then gradually increased as the ratio increased further. The total surface area ranged from 626 m^2 g^{-1} for HY-15.9 to 748 m^2 g^{-1} for HY-250 and HY-680.

3.2. IR measurements of pyridine adsorption

We determined the acid amount and strength of HY-5.6 and USY zeolites using IR measurements of adsorbed pyridine. Fig. 1 shows the IR spectra of adsorbed pyridine on HY-5.6 and USY zeolites at 423 K. The 1545 cm^{-1} band is assigned to the ν_{19b} vibration mode of pyridinium ions adsorbed on the Brønsted acid sites, and the 1455 cm^{-1} band to the ν_{19b} mode of coordinated pyridine on the Lewis acid sites [15]. The amounts of the Brønsted acid and Lewis

Table 1
Physical properties of HY-5.6 and USY zeolites used in this study

Zeolite [a]	Conditions for de-alumination			Unit cell constant (Å)	Crystallinity[b] (%)	Surface area[c] (m^2 g^{-1})	
	Concentration of HCl (mol dm^{-3})	Temperature (K)	Time (h)			Total	Mesopore
HY-5.6 [d]				24.59	96	720	19
HY-10.7 [e]				24.38	84	691	31
HY-15.0 [e]				24.29	88	662	71
HY-15.9	0.01	298	24	24.28	84	626	68
HY-25	0.03	298	24	24.28	84	653	78
HY-40	0.05	298	24	24.28	89	666	71
HY-78	0.1	298	24	24.28	86	690	83
HY-160	0.1	373	2	24.28	89	728	95
HY-250	0.5	373	2	24.26	81	748	97
HY-260	0.5	373	2	24.27	86	746	86
HY-680	2.0	373	2	24.23	76	748	96

[a]The number represents the SiO_2/Al_2O_3 ratio determined by ICP analysis.
[b]Calculated from the average area of 533 and 642 reflections using NaY as the reference.
[c] Total and mesopore surface areas were calculated using BET-plots and *t*-plots, respectively.
[d] Prepared by ion-exchange of NaY.
[e] As received.

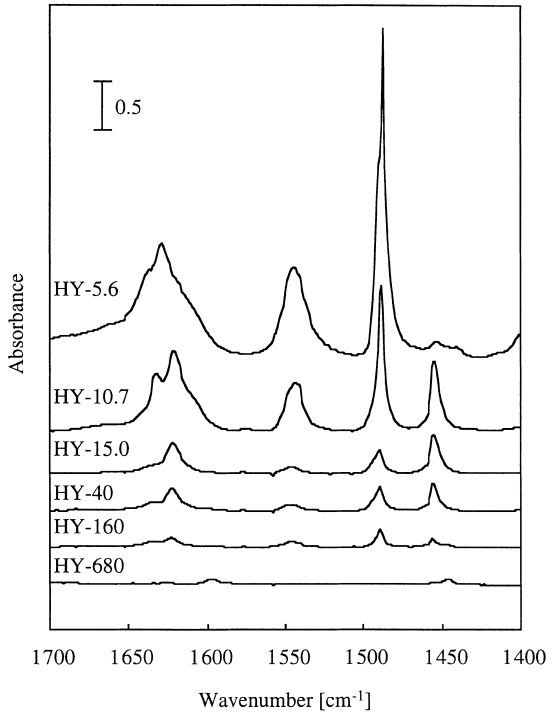

Fig. 1. IR spectra of pyridine adsorbed on HY-5.6 and USY zeolites after adsorption of pyridine (4 Torr) and desorption at 423 K.

acid sites were estimated from the integrated absorbance of both bands using the integrated molar extinction coefficients (1.67 cm μmol^{-1} for the 1545 cm^{-1} band and 2.22 cm μmol^{-1} for the 1455 cm^{-1} band) reported in the literature [16]. The acid strength was estimated from the desorption temperature (T_d) of the adsorbed pyridine. Fig. 2(a) and (b) show the amounts of Brønsted acid and Lewis acid sites, respectively, having acid strength of T_d higher than 423 K (○), 573 K (□), and 723 K (△). The Brønsted sites having acid strength of Td higher than 423 K significantly decreased when the SiO_2/Al_2O_3 ratio increased from 5.6 to 15.0, and decreased with further increase in the ratio from 15.0 to 680 although the amount of sites was extremely small. In contrast, the Lewis sites having acid strength of T_d higher than 423 K peaked at the SiO_2/Al_2O_3 ratio of 10.7, gradually decreased with an increase in the ratio, and completely disappeared for HY-680. A similar trend was seen for both the Brønsted sites and Lewis sites having acid strength of T_d higher than 573 K. The result of T_d higher than

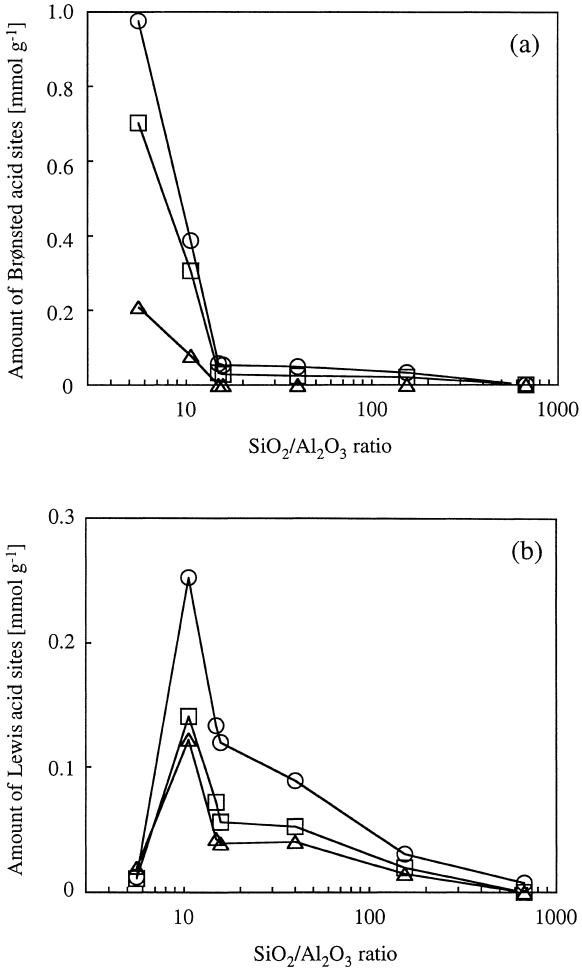

Fig. 2. Amounts of (a) Brønsted acid sites and (b) Lewis acid sites having acid strength of pyridine desorption temperature higher than 423 K (○), 573 K (□), and 723 K (△) for HY-5.6 and USY zeolites as a function of SiO_2/Al_2O_3 ratio.

723 K showed that strong Lewis acid sites existed on the surface of USY zeolites, even when the SiO_2/Al_2O_3 ratio exceeded 15.0.

3.3. *Tetralin hydrogenation over Pd–Pt/USY catalysts*

The time course for the conversion of tetralin and that for the selectivities of decalins (the sum of *trans*- and *cis*-decalin) and decalin isomers ($C_{10}H_{18}$ compounds except for decalins, such as methylbicyclo[0.3.4]nonanes and dimethylbicyclo[0.3.3]octanes)

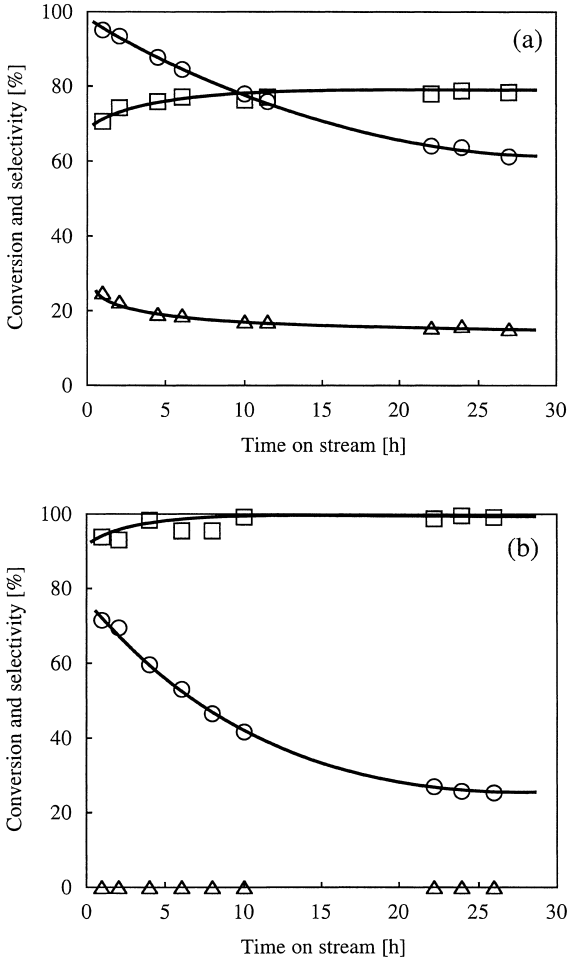

Fig. 3. Time courses for tetralin conversion (○), and for the selectivities of decalins (□) and decalin isomers (△) for the hydrogenation of tetralin in the presence of DBT over (a) Pd– Pt/HY-40 and (b) Pd–Pt/HY-680 catalysts. Total amount of metal loading = 1.2 wt.%; mole ratio Pd : Pt = 4. Reaction conditions: temperature, 553 K; hydrogen pressure, 3.9 MPa; WHSV, 16 h^{-1}.

are shown in Fig. 3(a) and (b) for the Pd–Pt/HY-40 and Pd–Pt/HY-680 catalysts, respectively. For both catalysts, the conversion gradually decreased with time on stream (t). The degree of deactivation for the Pd–Pt/HY-40 catalyst was much less than that for Pd–Pt/HY-680 (Fig. 3(a) and (b)). During the hydrogenation reaction, the products derived from tetralin were only *trans*- and *cis*-decalin for the Pd–Pt/HY-680 catalyst. In contrast, for Pd–Pt/HY-40, isomerization, hydrocracking, and polymerization of tetralin and decalins occurred as well as the hydrogenation of tetralin. Products other than decalins were decalin isomers, alkylcycloalkanes, gaseous hydrocarbons, and tetralin dimers and their hydrogenated derivatives for the Pd–Pt/HY-40 catalyst. Furthermore, this catalyst caused the hydrocracking of *n*-hexadecane. For both catalysts, the conversion of DBT reached 100%. For the Pd–Pt/HY-680 catalyst, the liquid products derived from DBT were bicyclohexyl and cyclohexylbenzene (biphenyl was not produced). On the contrary, for the Pd–Pt/HY-40 catalyst, only a small amount of bicyclohexyl was detected. The remaining products were the cracked ones. In the present study, however, it was difficult to distinguish the cracked products of DBT from those of tetralin.

Table 2 lists the results for the conversion and the selectivity at $t = 24$ h, and for the metal dispersion for the Pd–Pt catalysts supported on HY-5.6 and USY zeolites. The dispersion ranged from 0.30 for Pd–Pt/HY-5.6 to 0.52 for Pd–Pt/HY-78. The conversion increased as the SiO_2/Al_2O_3 ratio increased to 40, but decreased as the ratio increased further. We previously confirmed that the kinetics of the tetralin hydrogenation was first-order in tetralin content [13]. We therefore expressed the tetralin hydrogenation activity by a first-order rate constant per exposed surface metal atom defined as

$$k = \ln\left[\frac{1}{1-X}\right]\frac{F}{MWN}$$

where X is the conversion of tetralin into decalins, F is the flow rate of the liquid feed (4 g h^{-1}), M is the molecular weight of the feed (186.4 g mol^{-1}), W is the weight of catalyst (0.25 g), and N is the number of exposed surface metal atoms per weight of catalyst (mole per gram) obtained from the metal dispersion. Fig. 4 shows k at $t = 24$ h as a function of SiO_2/Al_2O_3 ratio. The activity of the Pd–Pt/HY-5.6 and Pd–Pt/USY catalysts strongly depended on the SiO_2/Al_2O_3 ratio of zeolites: The activity first increased with the increase in the SiO_2/Al_2O_3 ratio, peaked when the ratio was in the 15.0–40 range, and then gradually decreased as the ratio further increased to 680.

To evaluate the degree of deactivation, we also defined the relative activity as the ratio of k at $t = 24$ h to k at $t = 1$ h, and then plotted it against the SiO_2/Al_2O_3 ratio in Fig. 5. The relative activity showed behavior similar to the activity, peaking at the

Table 2
Conversion and selectivity for the hydrogenation of tetralin in the presence of DBT over Pd–Pt catalysts supported on HY-5.6 and USY zeolites[a]

Catalyst[b]	Dispersion[c]	Conversion (%)	Selectivity (%)			
			Decalins[d]	Decalin isomers[e]	Cracked products[f]	Polymers[g]
Pd–Pt/HY-5.6	0.30	16.2	67.1 (1.13)	16.2	9.0	7.7
Pd–Pt/HY-10.7	0.37	44.7	73.5 (0.78)	15.6	9.3	1.6
Pd–Pt/HY-15.0	0.34	56.4	68.2 (0.79)	15.2	13.7	2.9
Pd–Pt/HY-15.9	0.35	48.1	73.4 (0.89)	19.2	5.2	2.2
Pd–Pt/HY-25	0.49	61.3	78.3 (0.81)	16.5	2.3	2.9
Pd–Pt/HY-40	0.48	63.5	78.9 (0.80)	15.9	2.3	2.9
Pd–Pt/HY-78	0.52	56.3	76.5 (0.81)	20.0	1.9	1.6
Pd–Pt/HY-160	0.51	43.3	75.0 (0.78)	21.6	–	3.4
Pd–Pt/HY-250	0.39	29.0	86.0 (2.26)	11.1	0.8	2.1
Pd–Pt/HY-260	0.31	22.2	84.2 (2.11)	12.5	1.4	1.9
		25.2	86.3 (2.10)	11.1	0.3	2.3
Pd–Pt/HY-680	0.43	25.7	99.7 (2.77)	–	–	0.3

[a] Reaction conditions: 553 K; hydrogen pressure, 3.9 MPa; time on stream, 24 h.
[b] Total amount of metal loading, 1.2–1.3 wt.%; mole ratio Pd : Pt = 4.
[c] Determined from CO adsorption.
[d] Sum of *trans*- and *cis*-decalin. Numbers in parentheses are the *trans*-decalin/*cis*-decalin ratios.
[e] $C_{10}H_{18}$ compounds other than decalins.
[f] Alkylcycloalkanes, alkylbenzens, and gaseous hydrocarbons.
[g] Major products are tetralin dimers and their hydrogenated derivatives.

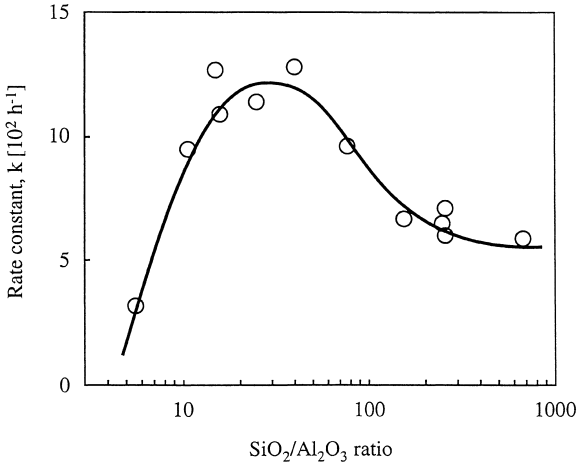

Fig. 4. Effect of the SiO_2/Al_2O_3 ratio of zeolites on the activity for the hydrogenation of tetralin in the presence of DBT over Pd–Pt/HY-5.6 and Pd–Pt/USY catalysts. Total amount of metal loading = 1.2–1.3 wt.%; mole ratio Pd : Pt = 4. Reaction conditions: Temperature, 553 K; hydrogen pressure, 3.9 MPa; WHSV, 16 h^{-1}; time on stream, 24 h.

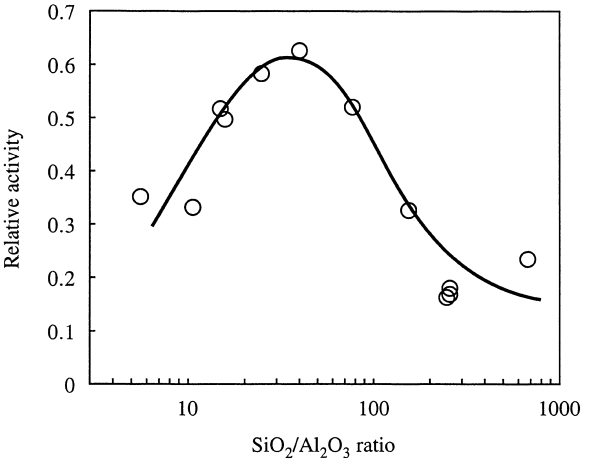

Fig. 5. Effect of the SiO_2/Al_2O_3 ratio of zeolites on the relative activity for the hydrogenation of tetralin in the presence of DBT over Pd–Pt/HY-5.6 and Pd–Pt/USY catalysts. Relative activity is the ratio of k at $t = 24$ h to k at $t = 1$ h.

SiO_2/Al_2O_3 ratio of 40. This means that the Pd–Pt/HY-40 catalyst had the smallest deactivation among the catalysts studied here.

As shown in Table 2, the selectivity of decalins at $t = 24$ h only slightly depended on the SiO_2/Al_2O_3 ratio (selectivity ranged from 67% for Pd–Pt/HY-5.6 to 79% for Pd–Pt/HY-40) when this ratio was below 160, but significantly increased (to higher than 99%)

when this ratio exceeded 160. The *trans*-decalin/*cis*-decalin ratio at $t = 24$ h was in the range from 0.7 to 0.8 when the SiO_2/Al_2O_3 ratio was below 160, except for the *trans*-decalin/*cis*-decalin ratio of 1.1 for Pd–Pt/HY-5.6. On the other hand, the *trans*-decalin/*cis*-decalin ratio tended to increase to 2.8 when the SiO_2/Al_2O_3 ratio increased to 680. The increase in the *trans*-decalin/*cis*-decalin ratio with an increase in the SiO_2/Al_2O_3 ratio is also reported for the hydrogenation of naphthalene over Pd catalysts supported on H-mordenite [17]. The selectivity of hydrocracked products generally decreased with an increase in the SiO_2/Al_2O_3 ratio.

4. Discussion

4.1. Structure and acidity of USY zeolites

The unit cell constant decreased from 24.59 to 24.28 Å when the SiO_2/Al_2O_3 ratio was increased from 5.6 to 15.9 (Table 1). However, no changes in the constant were observed when the SiO_2/Al_2O_3 ratio was further increased from 15.9 to 160. This means that the aluminum content in zeolite framework is constant although the SiO_2/Al_2O_3 ratios varies from 15.9 to 160. In contrast, the amount of Brønsted acid sites as well as Lewis acid sites decreased with this increase in the SiO_2/Al_2O_3 ratio from 15.9 to 160 (Figs. 1 and 2), although the amount of the Brønsted sites was extremely small. In the case of USY zeolites, the Lewis acid sites are probably due mostly to non-framework aluminum species such as $[AlO]^+$ [18,19]. On the other hand, a small amount of amorphous SiO_2–Al_2O_3 phase formed by partial destruction of zeolite framework during de-alumination, may contribute to the Brønsted acid sites for USY with the SiO_2/Al_2O_3 ratio of 15.9 to 160. This speculation is supported by the decrease in the crystallinity. Furthermore, it is reported that $Al(OH)_2^+$ species formed from $[AlO]^+$ and water function as a Brønsted acid site [19]. Thus, the decrease in the amount of the Brønsted acid sites associated with the increase in the SiO_2/Al_2O_3 ratio from 15.0 to 160 may be explained by the decrease in such an amorphous phase or $Al(OH)_2^+$ species.

On the other hand, the unit cell constant decreased from 24.28 to 24.23 Å when the SiO_2/Al_2O_3 ratio was further increased from 160 to 680. Therefore, the elimination of aluminum in the zeolite framework is responsible for the decrease in the amount of the Brønsted acid sites associated with the increase in the ratio from 160 to 680.

4.2. Sulfur tolerance of Pd–Pt/USY catalysts

For the Pd–Pt/HY-40 catalyst, the acid sites (mostly Lewis acid sites, Fig. 2) in HY-40 allowed isomerization, hydrocracking, and polymerization to proceed (Fig. 3(a) and Table 2). However, the degree of deactivation was much smaller and a high hydrogenation activity was maintained even after 24 h. On the other hand, the hydrogenation selectivity reached almost 100% for the Pd–Pt/HY-680 catalyst (Fig. 3(b) and Table 2), because there were no acid sites on the surface of HY-680. However, the deactivation was greater and the activity at $t = 24$ h became lower, compared with Pd–Pt/HY-40. When DBT is not present in the feed, no deactivation is detected, even after 24 h [13]. This means that the deactivation is caused by the presence of DBT, and that the influence of coke deposition on the deactivation is small.

For the Pd–Pt catalysts supported on HY-5.6 and USY zeolites, both the tetralin hydrogenation activity and the degree of deactivation depended on the SiO_2/Al_2O_3 ratio of zeolites, and both peaking at the ratio of around 40 (Figs. 4 and 5). These results show that Pd–Pt/HY-40 catalyst has the highest sulfur tolerance of the catalysts studied here, and is able to maintain high activity even after 24 h. Next, we discuss the reason that bimetallic Pd–Pt particles have a high sulfur tolerance and high activity when supported on USY with the SiO_2/Al_2O_3 ratio of 15.0–40.

It is well known that acidic protons on a zeolite reduce the electron density of a supported metal, thereby weakening the bonding energy between an electron-deficient metal and an electron-acceptor sulfur [20–22]. According to this explanation, the sulfur tolerance of the supported metal would increase as the Brønsted acidity of zeolite increases. For the USY zeolites with a SiO_2/Al_2O_3 ratio of 15.0 or above, the amount of Brønsted acid sites was extremely small (Fig. 2(a)), while strong Lewis acid sites existed on the surface of these zeolites (Fig. 2(b)). If the Lewis acid sites as well as Brønsted acid sites function as electron-acceptor sites of the metals, then the decrease

in both the activity and the sulfur tolerance when the SiO_2/Al_2O_3 ratio increases from around 15.0–40 to 680 (Figs. 4 and 5) could be explained as follows: Pd–Pt supported on HY-15.0 or HY-40 becomes electron deficient due to the strong Lewis acidity of zeolites. As a result, the Pd–Pt/HY-15.0 or Pd–Pt/HY-40 catalyst has a high sulfur tolerance and high activity for the hydrogenation of tetralin. On the other hand, there were no acid sites on the surface of HY-680 zeolite, and thus, Pd–Pt on HY-680 is easily poisoned by sulfur, thereby resulting in low sulfur tolerance and low hydrogenation activity. That is to say, the decrease in both the activity and the sulfur tolerance of Pd–Pt/USY catalysts when the SiO_2/Al_2O_3 ratio increases from 15.0–40 to 680 could be due to the decrease in the amount of electron-deficient Pd–Pt resulting from the decrease in Lewis acidity.

We cannot exclude the possibility that the decrease in activity with the increase in the SiO_2/Al_2O_3 ratio is due to the agglomeration of Pd–Pt particles. When DBT is not present in the feed, sintering or agglomeration of Pd–Pt is absent, or at an undetectable level, because we observed no deactivation. However, agglomeration of metals might occur when either DBT or hydrogen sulfide is present in the reaction atmosphere. The melting point of Pd and Pt is 1828 and 2042 K, respectively, whereas that of eutectic compounds of Pd–PdS and Pt–PtS is 896 and 1513 K, respectively [23]. This means that the melting points are lower after the formation of eutectic compounds of metals and metal sulfides. Thus, when Pd and Pt metals are partly sulfided, the mobility of Pd and Pt atoms would increase and Pd–Pt particles would more easily agglomerate. Acid sites may act as chemical anchors of supported metals, thereby suppressing the agglomeration of metals and keeping the metals highly dispersed [22,24]. According to this idea, the agglomeration of Pd–Pt on USY zeolites would become easier and the hydrogenation activity lower as the acidity of USY zeolites decreases with an increase in the SiO_2/Al_2O_3 ratio. Thus, the decrease in activity of Pd–Pt/USY catalysts when the SiO_2/Al_2O_3 ratio increases from 15.0–40 to 680 may be associated with the increase in the agglomeration of Pd–Pt particles resulting from the decrease in acidity.

The activity and the sulfur tolerance of Pd–Pt may relate to the acidity of USY zeolites. However, the activity and the sulfur tolerance of Pd–Pt/HY-5.6 and Pd–Pt/HY-10.7 were lower than those of Pd–Pt/HY-15.0 or Pd–Pt/HY-40, although larger amounts of Brønsted acid and Lewis acid sites existed on the surface of HY-5.6 and HY-10.7, respectively. This means that changes in the activities of the Pd–Pt catalysts cannot be explained simply by the effect of the acidity of zeolites. We previously examined the effect of pore diffusional resistance on the tetralin hydrogenation activity of Pd–Pt/HY-5.1 under the same reaction conditions used in this study, except WHSV $= 8\ h^{-1}$, and reported the effectiveness factor for the 22/48 mesh-size catalyst to be 0.69 [13]. This result indicates that the hydrogenation activity is somewhat affected by the pore diffusional resistance. Recently, for the hydrogenation of naphthalene in the presence of benzothiophene, Song et al. [25] have reported that Pd becomes highly sulfur tolerant when Pd is supported on de-aluminated mordenite with large surface area in the mesopore region. They have suggested that one possible reason for the high sulfur tolerance of the catalyst is the ease of the intrapore and out-of-pore diffusion processes. In this study, the mesopore surface areas of HY-5.6 and HY-10.7 were 19 $m^2\ g^{-1}$ and 31 $m^2\ g^{-1}$ (Table 1), respectively, and were smaller compared with those of USY zeolites with a SiO_2/Al_2O_3 ratio of 15.0 or above. From these results, the diffusion of tetralin into the micropores of Y-type zeolite may be slow in the presence of *n*-hexadecane, and Pd–Pt particles existed on the mesopores of the USY zeolite crystallites may be the major contributor to the hydrogenation of tetralin, although tetralin is small enough to enter the supercages of Y-type zeolite with respect to the molecular size. The Pd–Pt/HY-5.6 and Pd–Pt/HY-10.7 catalysts could be potentially highly sulfur tolerant, because these catalysts have large amounts of acid sites. However, the amount of effective Pd–Pt on the Pd–Pt/HY-5.6 and Pd–Pt/HY-10.7 catalysts is probably smaller, and hence, these catalysts showed the lower activity and lower sulfur tolerance, compared with the Pd–Pt/HY-15.0 or Pd–Pt/HY-40 catalysts.

5. Conclusions

Hydrogenation of tetralin in the presence of dibenzothiophene was done over bimetallic Pd–Pt (mole ratio Pd : Pt = 4 : 1) catalysts supported on HY and

USY zeolites, whose SiO_2/Al_2O_3 ratio was widely varied from 5.6 to 680. The activity and the sulfur tolerance first increased with the increase in the SiO_2/Al_2O_3 ratio of zeolites, peaked when the ratio was in the 15.0–40 range, and then gradually decreased as the ratio further increased to 680. The decrease in both the activity and the sulfur tolerance of Pd–Pt/USY catalysts when the SiO_2/Al_2O_3 ratio increases from 15.0–40 to 680 may be primarily due to the decrease in the amount of electron-deficient Pd–Pt resulting from the decrease in Lewis acidity. On the other hand, the low activities of Pd–Pt/HY and Pd–Pt/USY ($SiO_2/Al_2O_3 = 10.7$) catalysts are probably because of the pore diffusional limitations.

Acknowledgements

We thank Dr. Y. Miki of the National Institute of Materials and Chemical Research for the GC-MS measurements and for helpful discussions. We also thank Catalysts and Chemicals Industries Co. for the ICP measurements.

References

[1] A. Stanislaus, B.H. Cooper, Catal. Rev. Sci. Eng. 36 (1994) 75.
[2] B.H. Cooper, B.B.L. Donnis, Appl. Catal. A 137 (1996) 203.
[3] C.H. Bartholomew, P.K. Agarwal, J.R. Katzer, Adv. Catal. 31 (1982) 135.
[4] J. Barbier, E. Lamy-Pitara, P. Marecot, J.P. Boitiaux, J. Cosyns, F. Verna, Adv. Catal. 37 (1990) 279.
[5] A. Arcoya, X.L. Seoane, N.S. Figoli, P.C. L'Argentiere, Appl Catal. 62 (1990) 35.
[6] M. Koussathana, D. Vamvouka, H. Economou, X. Verykios, Appl. Catal. 77 (1991) 283.
[7] S.D. Lin, C. Song, Catal. Today 31 (1996) 93.
[8] S.M. Kovach, G.D. Wilson, US Patent 3 943 053, 1974.
[9] J.K. Minderhoud, J.P. Lucien, Eur. Patent 303 332, 1988.
[10] S.G. Kukes, F.T. Clark, P.D. Hopkins, L.M. Green, US Patent 5 151 172, 1991.
[11] T.B. Lin, C.A. Jan, J.R. Chang, Ind. Eng. Chem. Res. 34 (1995) 4284.
[12] M. Sugioka, F. Sado, Y. Matsumoto, N. Maesaki, Catal. Today 29 (1996) 255.
[13] H. Yasuda, Y. Yoshimura, Catal. Lett. 46 (1997) 43.
[14] H. Stach, U. Lohse, H. Thamm, W. Schirmer, Zeolites 6 (1986) 74.
[15] J.W. Ward, J. Catal. 9 (1967) 225.
[16] C.A. Emeis, J. Catal. 141 (1993) 347.
[17] A.D. Schmitz, G. Bowers, C. Song, Catal. Today 31 (1996) 45.
[18] D.W. Breck, G.W. Skeels, in: Proc. 6th Int. Congr. Catalysis, 1977 p. 645.
[19] P.A. Jacobs, H.K. Beyer, J. Phys. Chem. 83 (1979) 1174.
[20] R.A. Dalla Betta, M. Boudart, in: Proc. 5th Int. Congr. Catalysis, 1973 p. 1329.
[21] P. Gallezot, Catal. Rev. Sci. Eng. 20 (1979) 121.
[22] P. Gallezot, G. Bergeret, in: E.E. Petersen, A.T. Bell (Eds.), Catalyst Deactivation, Marcel Dekker, New York, 1987, p. 263.
[23] T.B. Massalski, H. Okamoto, P.R. Subramanian, L. Kacprzak (Eds.), Binary Alloy Phase Diagrams, 2nd ed., vol. 3, ASM International, 1990.
[24] W.M.H. Sachtler, Z. Zhang, Adv. Catal. 39 (1993) 129.
[25] C. Song, A.D. Schmitz, Energy and Fuels 11 (1997) 656.